

**A STUDY OF AN INDUSTRIAL GAS TURBINE FUEL SPRAY INJECTOR IN A CROSS-FLOW.
CHARACTERISATION AND COMPARISONS WITH CFD PREDICTIONS.**

by

Nigel Wilbraham[‡], Victoria Sanderson[‡], Khawar Syed[‡], Marios S Christodoulou[†], Mark D Turrell^{*}, Philip J Stopford^{*}

[†]Scitek Consultants Ltd

[‡]Demag Delaval Industrial Turbomachinery Ltd

^{*}ANSYS CFX

ABSTRACT

The interest in low emissions combustion technology for premixed liquid fuelled devices has increased in recent years due to more power generation companies demanding greater fuel flexibility. Such devices can rely increasingly on the process of secondary atomization to promote greater fuel to air mixing. It is quickly evident when designing such devices that there are limited analytical tools, and those that do exist require some form of validation.

This study focuses on providing good quality experimental data that can validate CFD modelling of droplet dynamics and break-up in cross-flows. The data gathered is being used to develop such secondary break-up models in CFD.

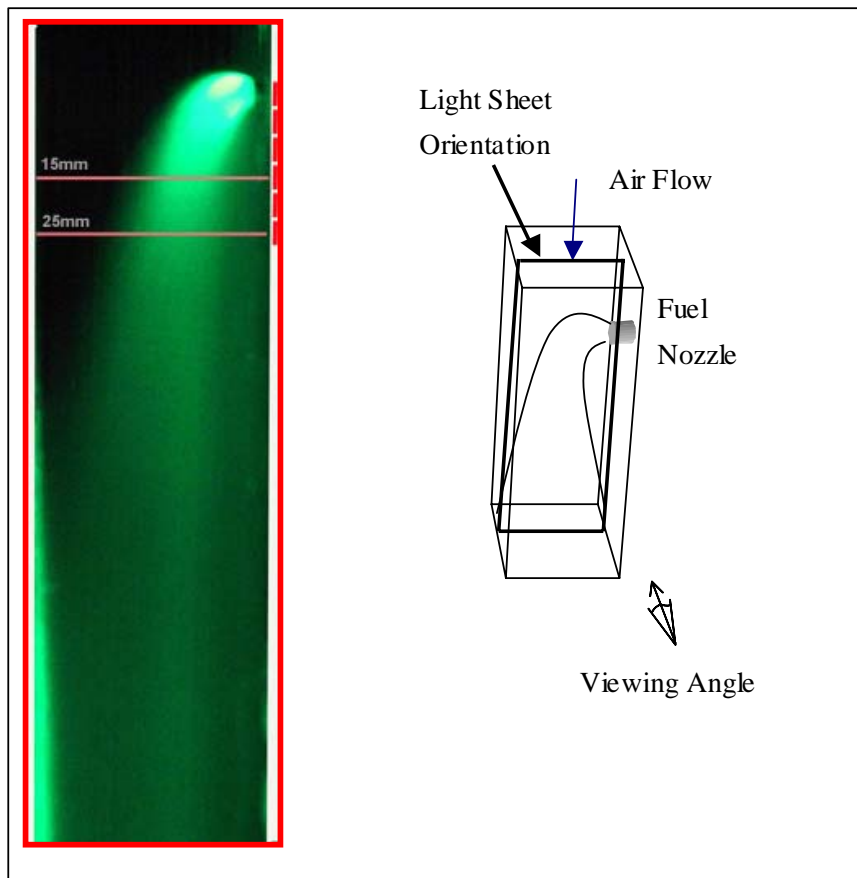


Figure 1. Laser light sheet image of the spray in its cross-stream duct

1. INTRODUCTION

Stationary gas turbine NO_x emissions have been reduced significantly for premium gaseous fuel over the last few years, and it is likely that these limits will be reflected for liquid fuel operation in the future. To meet the challenge, a design of premixing liquid fuelled burner is needed that will cover the range of operating loads expected. Such systems can involve significant amounts of secondary atomisation in their rapid vaporisation designs. Whilst it is recognised that progressive secondary atomisation occurs in all fuel sprays, the degree of secondary atomisation is significantly higher in a cross-stream duct. The break-up time is much reduced and consequently the amount of premixing is greater.

For a low NO_x liquid fuel burner, the fuel spray droplets must be evaporated quickly to enable further mixing of the vaporised phases with additional combustion air. The process of atomisation and the trajectories of the associated droplets are critical to the vaporisation phase mixing. Increasingly, the use of secondary atomisation in burners is seen as an important part of the process. However, modelling of the secondary break-up of droplets is not readily done in most CFD packages, and those that do are limited in their capability and have almost no realistic validation data.

A simplex atomiser has been subjected to detailed PDPA measurement both with and without a cross-stream airflow. These datasets provide a first order approximation to the primary and secondary atomisation processes occurring in a liquid fuelled premixing duct. The primary atomisation process associated with the normal operation of an atomiser can be measured independently from the secondary process, which gives a means of validating to a first order, any future implementation in CFD models.

A purpose built airflow rig, producing a uniform flow profile was used as the cross-stream generator for the fuel spray. Initially, flow visualisation using laser light sheet was used to establish the shape of the fuel spray with and without a cross-stream flow. Example images are shown in Figure 1 and Figure 6. Detailed spray measurements using a PDPA system were then carried out to obtain comprehensive mapping of the spray velocity and size at two planes downstream of the nozzle. A 10x10 measurement grid at 3mm pitch was used and at each plane, measurements were carried out at three airflow velocities. Typical air velocities and volume mean (D30) results are shown in Figure 8 and Figure 9.

From the measurements, it was established that with increasing airflow velocity, the size of the droplets was reduced. This was a result of droplet secondary break-up when subjected to higher aerodynamic shear at the increased airflow velocities. It was also deduced that the body of the spray acts as a bluff body to the air stream and a wake is produced close to the root of the spray. Close to the root of the spray, only small droplets are present the larger ones taking a longer trajectory, and thus only found towards the outer plane of the flow rig. The hollow cone structure of the spray is also broken down and a horseshoe-like structure is formed. The datasets reveal secondary atomisation and its interaction with the global spray dynamics, which is the key aspect of the work, which will drive future designs.

At present, work is underway using a commercial CFD code (CFX5.6 [2]) to model the airflow and spray with the intention of comparing predictions with the experimental measurements. A realistic definition of the spray boundary condition is of great importance in the modelling of liquid fuel jets. These experiments were specifically design to provide accurate definition of both the air and spray boundary condition. The size distribution and volume flux of the unconfined spray measured by the PDPA (i.e. with no cross flow) has provided the spray boundary conditions to the CFD model. A secondary break-up model using correlations developed by Schmehl et al [1], based on Weber and Ohnesorge numbers, has been incorporated into the CFD Lagrangian droplet model. An assessment of the correlations and their influence on the predictions has been made.

This paper will disclose details of the experimental finding in the cross-flow rig. Preliminary results from the CFD analysis will be presented explaining the philosophy used in simulating the spray and analysing the results.

2. EXPERIMENTAL SETUP

Experimental work was carried out on the unconfined spray (i.e. not subjected to any cross-flow) to obtain the overall characteristics of a nozzle under different operating conditions. The nozzle was then placed in the cross-flow rig where more measurements were carried out. Each of the two experimental set-ups is outlined below.

All experiments were carried out at the Demag Delaval Industrial Turbomachinery Ltd spray facility in Lincoln where spray nozzles can be flowed under accurate control of fuel flow rates and temperatures. The liquid used for these tests is Castrol C which at the temperature of approx.30 deg C has properties similar to diesel. A schematic of this facility is shown in Figure 2 and incorporates a fuel re-circulation tank, fuel cooler and air extraction facility so that the fine airborne spray is directed in to the separator so that it is safe for the operators to be in close proximity of the rig and provides protection for the instrumentation.

2.1 UNCONFINED SPRAY – LIGHT SHEET, PDA, MALVERN

For the unconfined spray experiments, the nozzle was placed in a holder that was mounted on a 2-D traverse. Flow visualisation experiments were carried out using a light-sheet probe and a digital camera viewing the light sheet at right angles. For size distributions an Aerometric PDA (counter type) system was used at various locations in the spray and a Malvern particle sizing system (Mastersizer X) to obtain a size distribution integrated across the full width of the spray cone. A Schematic of the experimental set-up is shown in Figure 3.

2.2 CROSS FLOW RIG – LIGHT SHEET AND PDA

The cross flow rig was purposely built for these tests and incorporates three sliding glass panels that allow optical access for flow visualisation experiments. It incorporates a plenum chamber that was fed with compressed air at three locations (see **Figure 4**) that discharged into atmosphere via a squared cross section pipe that was 400mm long (i.e. outlet at ambient pressure and temperature). The plenum chamber was filled with wire-gauze to ensure uniform airflow within the 30mmx30mm cross pipe section, which provided the cross-flow to the fuel nozzle. Inside this section and close to the plenum chamber a honeycomb was used to remove any swirl in the flow entering from the plenum chamber. A pressure regulator and gauge controlled airflow velocity within the test section

The fuel nozzle was mounted on the non-glass side of the rig test-section that could be traversed in the vertical direction and thus moving the nozzle relative to the PDA measurement volume, which was fixed. The cross-flow rig was also mounted on a two-dimensional traverse that allowed movement in the horizontal plane. With this arrangement, movement of the nozzle in relation to the PDA probe volume could be achieved along the three orthogonal axes. In practice, the distance of the nozzle was fixed (Z-axes) and measurements were conducted on a 10x10 grid with 3mm. grid spacing (i.e., 30mm. by 30mm. planar traverse dimensions). This arrangement made the optical set-up of the PDA equipment quick and convenient.

Optical access to the area of interest was via a 10mm. gap (see Figure 4) in the cross-section of the rig, which allowed clear view of the flow at all times. The rig outlet was configured to be approximately 100mm. downstream from the measurement region of the test section. The excess fuel and air mixture exiting the outlet was impacting onto a porous metallic plate and into a settling chamber that was part of the Demag Delaval Industrial Turbomachinery Ltd spray facility (see **Figure 2**)

2.3 MOMENTUM SCALING

Momentum scaling was used to scale the air and fuel flow to match that of the engine running conditions. This is necessary since the spray facility is an isothermal atmospheric pressure facility. The maximum airflow achieved on the cross flow rig was used as the basis for all the scaling. For the atmospheric cross-flow rig, the maximum velocity that could be achieved was around 70m/s.

$$\left(\frac{\rho_{air} \times A_{air} \times V_{air}^2}{\dot{m}_{fuel}} \right)_{Engine} = \left(\frac{\rho_{air} \times A_{air} \times V_{air}^2}{\dot{m}_{fuel}} \right)_{Rig}$$

For maximum flexibility in rig airflows, it was necessary to try the minimum possible fuel flow for visually good atomisation. This fuel flow was then used to fix the scaled airflows for the testing. This procedure was necessary because the nozzle manufacturer could not supply a nozzle with a scaled flow-number.

For the unscaled nozzle flow number this flow was found to be 0.0055kg/s.

2.4 EXPERIMENTAL CONDITIONS (I.E. FUEL FLOW AND AIR SUPPLY)

Based on the Demag Delaval Industrial Turbomachinery Ltd, Typhoon 4.9 engine and using momentum scaling on a scaled fuel flow rate of 5.5g/s the equivalent air flow conditions for the cross flow rig, air-flow conditions were:

Test point 1	load produces a rig air flow of	= 66m/s
Test point 2	load produces a rig air flow of	= 53m/s
Test point 3	load produces a rig air flow of	= 40m/s

Thus, detailed flow and size mappings at all three conditions were obtained at two locations downstream of the fuel nozzle exit plane as shown in Figure 1.

2.5 CFD MODEL

A Computational Fluid Dynamics model has been created in CFX-5.7 [2] to simulate the behaviour of the spray within the experimental duct. The airflow field was computed on an unstructured tetrahedral mesh of 104,000 nodes while the spray droplets were simulated by the Lagrangian tracking model with 36,000 representative particles. The equation of droplet motion included buoyancy and drag forces. Droplets impacting on the duct walls were removed from the calculation. The effect of droplet distortion on drag and secondary break-up due to shear flow were modelled using the correlations of Schmehl et al. [1]. The gas flow and particle motion were coupled through the drag force and so the gas and particle calculations were iterated until convergence was achieved. The inlet airflow distribution and the initial particle size and velocity distribution were taken from the experimental measurements with a maximum droplet diameter of 215 microns.

3.0 RESULTS

3.1 UNCONFINED SPRAY

These tests were aimed at establishing the characteristics of the nozzle at different fuel flow rates so that the results serve as a reference for comparison with results from the cross flow rig but also for comparison with any future experimental programme where different nozzles may be used.

3.2 FLOW VISUALISATION

Images of the spray produced by the nozzle at two fuel flow rates are shown in Figure 5. The low fuel flow rate was at the scaled condition, which for this nozzle's flow number did not produce good atomisation something that is quite evident from the images. The higher flow rate of 10g/s is the correct flow rate for the flow number of the nozzle and as can be clearly seen this produced much finer atomisation. From the results it was evident that a lower flow number nozzle was needed so that at the scaled fuel flow rate the atomisation would have been, similar to that produced by the nozzle used here at 10g/s. However, such a nozzle was not available at the time of the work and the main interest of the results produced here are to serve as data that can be used for CFD validation. It is planned that more experiments will follow with a lower flow number fuel nozzle.

What is also evident from the images is that both have a hollow cone spray structure, which is characteristic for swirl type atomisers with most of the fuel being sprayed close to the edges of the spray cone.

3.3 SIZE MEASUREMENTS – MALVERN AND PDA

The Malvern instrument has a wider dynamic range than the PDA so the main purpose of using it was to establish the size distribution produced by the nozzle integrated across the full width of the spray cone. Results for the 5.5g/s fuel flow rate are shown in Figure 11 where it can be seen that very large droplets are produced that confirms what was observed from the flow visualisation images. These results clearly show that there is a very wide range of droplets produced which is a result of operating the nozzle outside its optimum flow rate condition.

Measurements with the PDA system confirmed (see **Figure 11**) in quantitative terms that the nozzle produces a hollow cone spray and that the largest droplets are confined to the outer edge of the spray cone. It was also measured that the swirl velocity produced by the nozzle is virtually zero which is indicative of the nozzle producing the hollow cone spray by wetting of a divergent conical outlet rather than by swirling the liquid to high swirl velocities.

In the configuration used, the PDA instrument had an upper particle diameter limit of 180 microns and therefore could not measure the very large droplets produced by the nozzle and therefore the interpretation of size results is somewhat limited. In future experiments it is intended to reduce the beam separation of the PDA so that the measured size range could be increased. This will enable direct comparisons of droplet size distributions between the two instruments with the aim to improve the accuracy of the droplet boundary conditions to the CFD model.

3.4 CROSS FLOW RIG

This rig formed the basis of a simple CFD simulation the geometry of which was very easy to generate a grid and thus allow more time to be devoted to modelling of the droplet break-up. The airflow velocity field was to be used as boundary conditions to the CFD model and this is discussed in the next section.

3.5 NO FUEL AIR SUPPLY VELOCITY PROFILE

The airflow velocity was measured using a pitot tube, which was traversed, across the flow area of the rig at a distance of 300mm from the inlet. At this location, a fully developed flow was expected, as it was 10 times the width of the rig. The results are shown in Figure 7 where it can be seen that the boundary layer was around 5mm thick and the flow producing 20 percent variability in the flatness of the velocity profile. These results were then used as inlet boundary conditions to the CFD model.

3.6 VELOCITY AND SIZE MEASUREMENTS

From the measurements made only a selected number of results are presented here

The airflow axial velocity component was produced by averaging the velocity of the smallest droplet size group (droplets smaller than 4 microns). Results are shown in Figure 8, which represent one location downstream of the nozzle at three air mass flow conditions. These results show that the fuel spray forms a blockage to the axial flow. The regions of highest axial velocity are close to the wall where the nozzle is mounted, as this is the region where the spray plume is thinnest and thus present the least blockage to the airflow. These results will be compared with the CFD results and the degree of agreement will be a measure of how well the CFD takes into account the exchange of momentum that takes place between airflow and the spray.

Figure 7 shows the volume mean diameter of the spray distribution measured at each point in the rig. It is clearly seen that close to the wall where the nozzle is mounted only the smallest droplets are found. With increasing distance from the nozzle wall as the size of the volume mean increases with the largest droplets found very close to the wall opposite the nozzle.

Figure 10 also shows the difference in the average velocity of the smallest droplets (below 4 microns) with the average velocity of droplets of 44 microns in size. Results show that there is a high shear either side of the main spray plume, which is consistent with the obstruction of the spray plume to the central airflow. These results will also form a measure of how well the CFD models the dynamics (drag coefficient etc) of the droplets.

4.0 COMPARISONS WITH CFD

The predicted droplet trajectories for Test Point 1 (mean air flow rate of 66 m/s) are shown in Figure 12. Some large droplets fail to break-up and impact the duct wall but most break-up to produce fragments that quickly become entrained in the gas flow. The duct flow therefore acts like a droplet size classifier as shown in Figure 12. By taking into account that the smaller droplets contribute most to light scattering then the CFD results show a similar spray profile to the laser light sheet image from the spray centre plane as shown in Figure 1. A detailed comparison with the gas and droplet velocity fields will be published elsewhere.

5.0 CONCLUSIONS

This study forms the first part of a programme that is aimed to improve the capability of CFD in modelling the secondary break-up and dynamics of fuel sprays so that it can be used with more confidence to predict more complex combustor geometry studies.

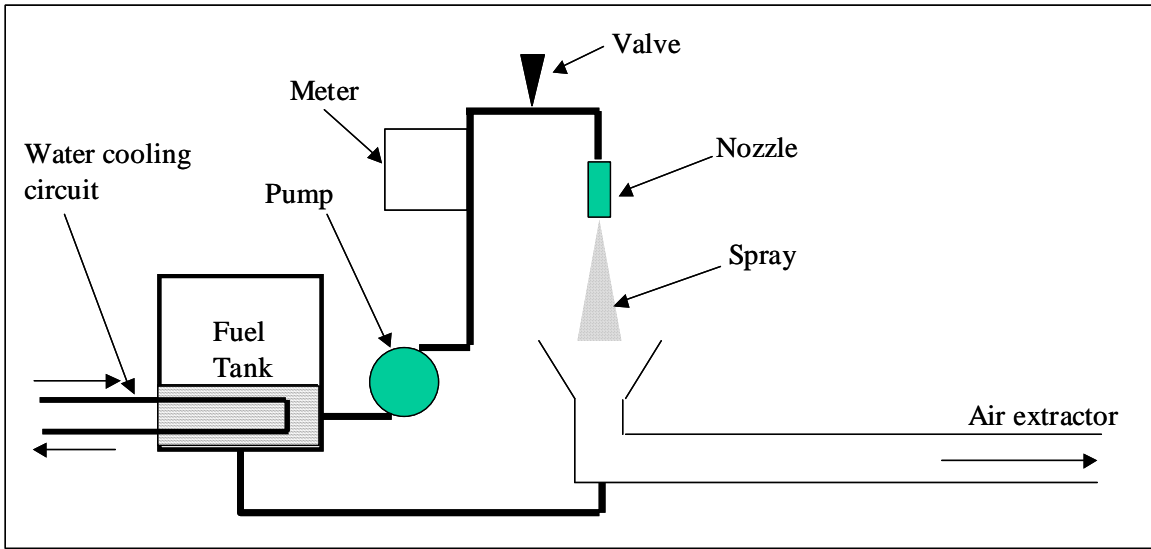


Figure 2. The Demag Delaval Industrial Turbomachinery, spray test facility

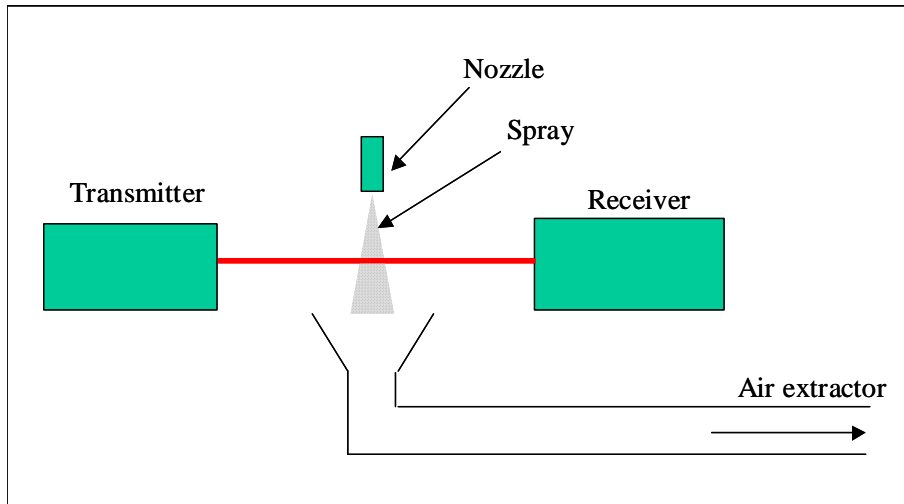


Figure 3. The Malvern Mastersizer-X configuration

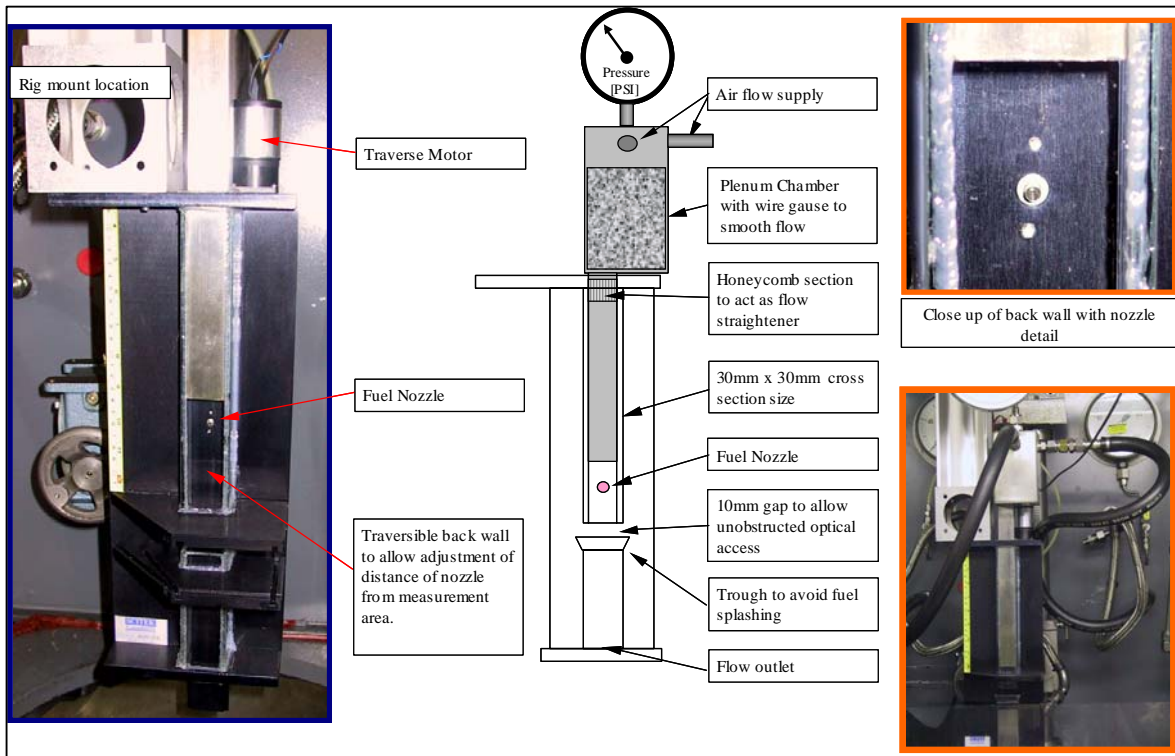


Figure 4. The cross-flow rig configuration.

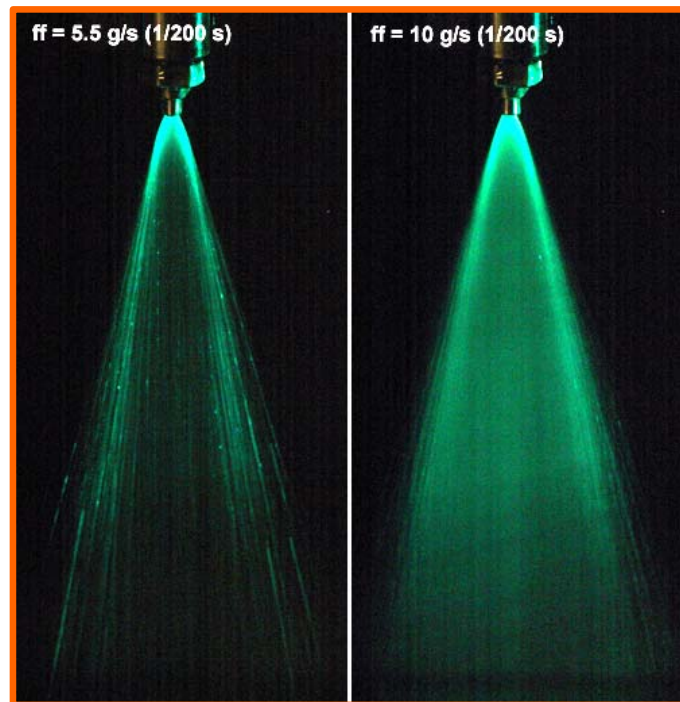


Figure 5. Flow visualisation of spray nozzle using laser sheet lighting at two fuel flow rates. Spray was unconfined with no forced airflow. Better atomisation takes place at higher fuel flow rate.

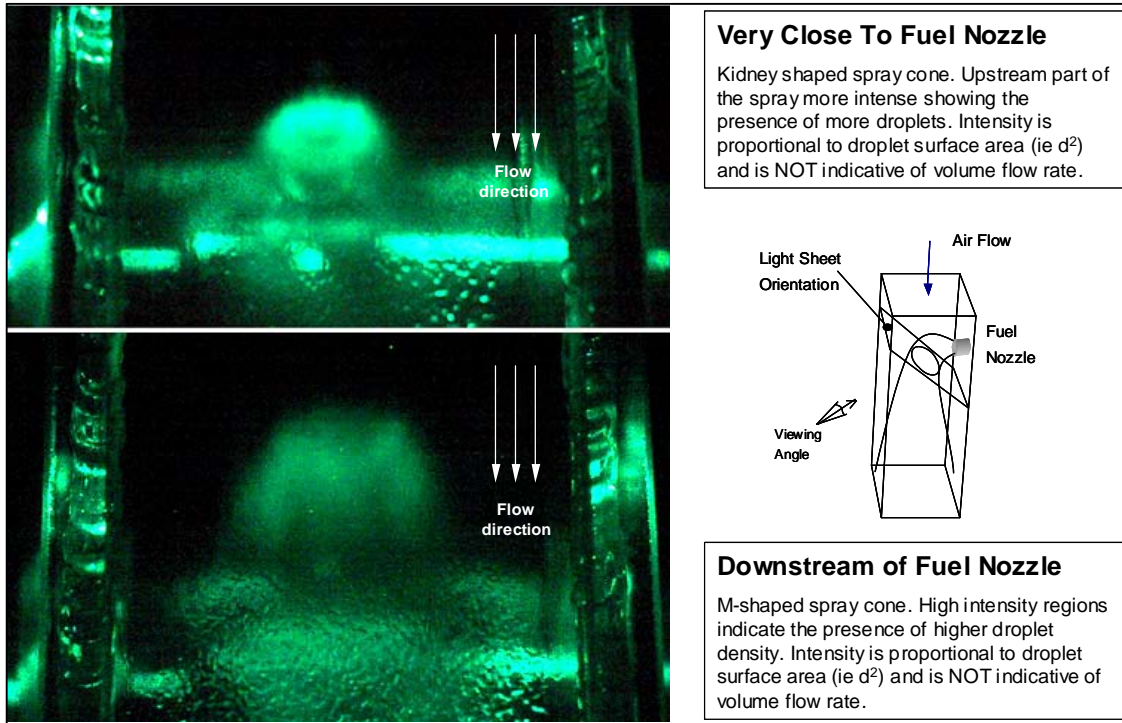


Figure 6. Flow visualisation of fuel spray in cross flow rig. Cross section pictures show the evolution of the hollow cone spray structure under the influence of the airflow.

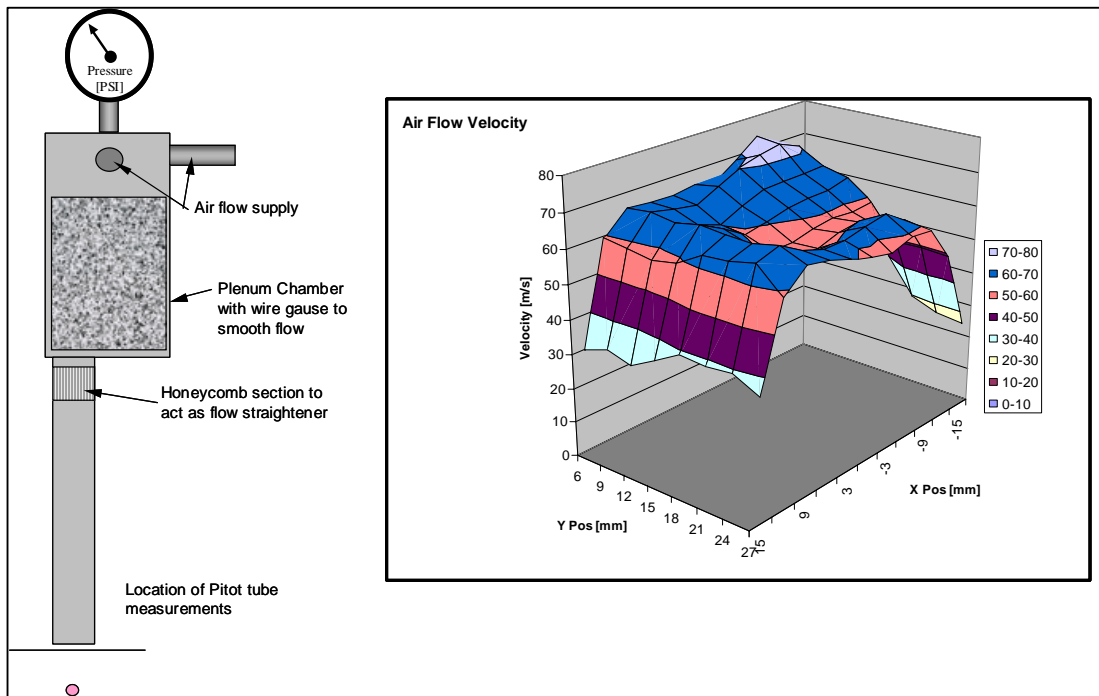


Figure 7. The air inlet velocity profile as measured using a pitot tube. The plot shows the wall boundary layer at either side. The X-wise traverse does not show the boundary layer since the traverse length did not cover the whole duct in that orientation.

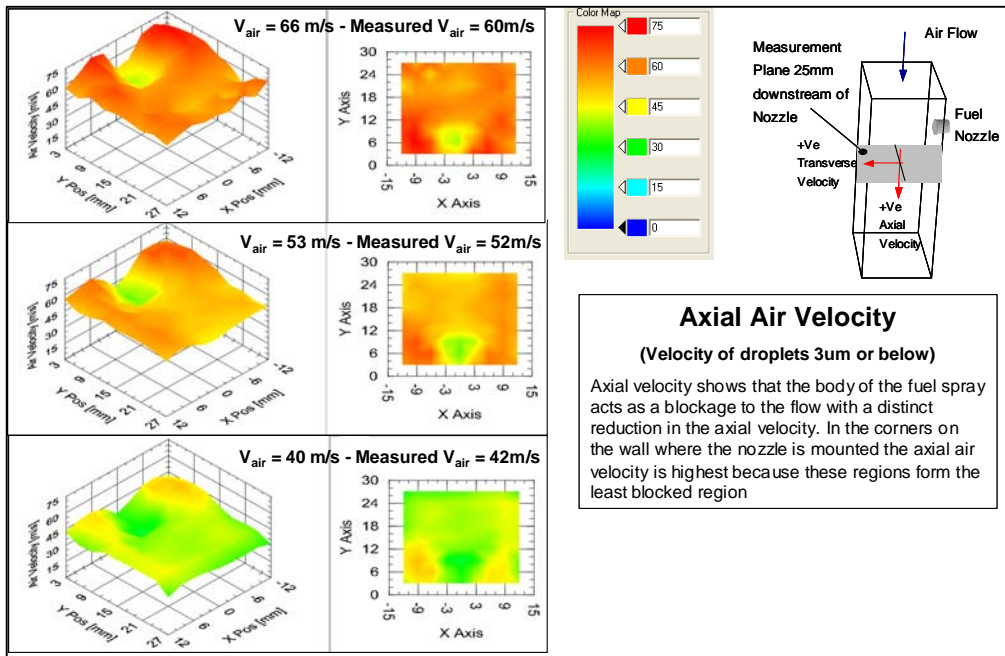


Figure 8. Axial airflow velocity map measured at three cross-stream velocities. Results show that the body of the fuel spray acts as a blockage to the flow with a distinct reduction in the axial velocity. In the corners on the wall where the nozzle is mounted, the axial air velocity is highest because these regions form the least blockage.

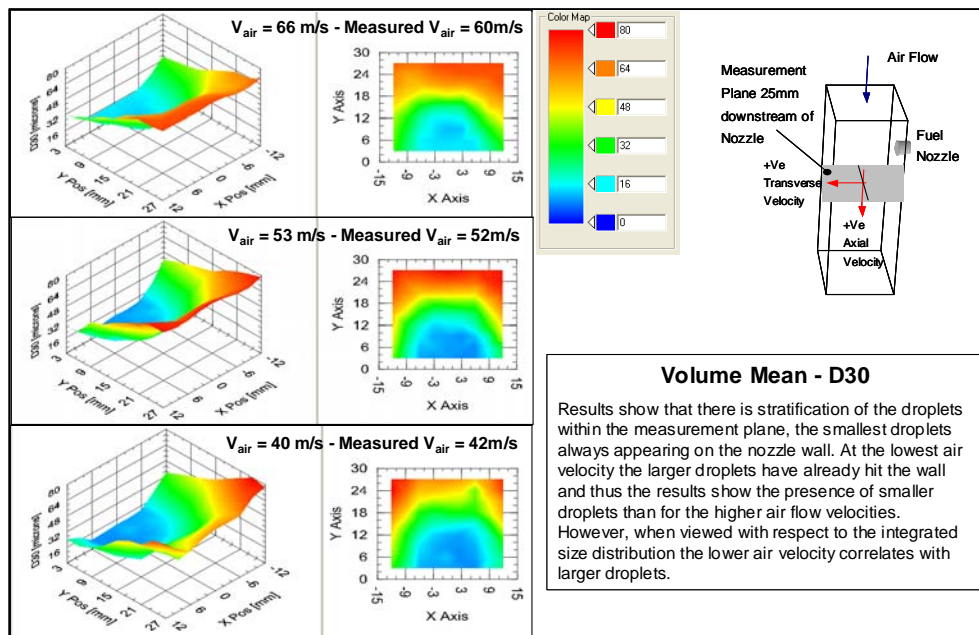


Figure 9. Volume Mean (D30). Results show that there is stratification of the droplets within the measurement plane, the smallest droplets always appearing on the nozzle wall. At the lowest air velocity, the larger droplets have already hit the wall and thus the results show the presence of smaller droplets than for the higher airflow velocities.

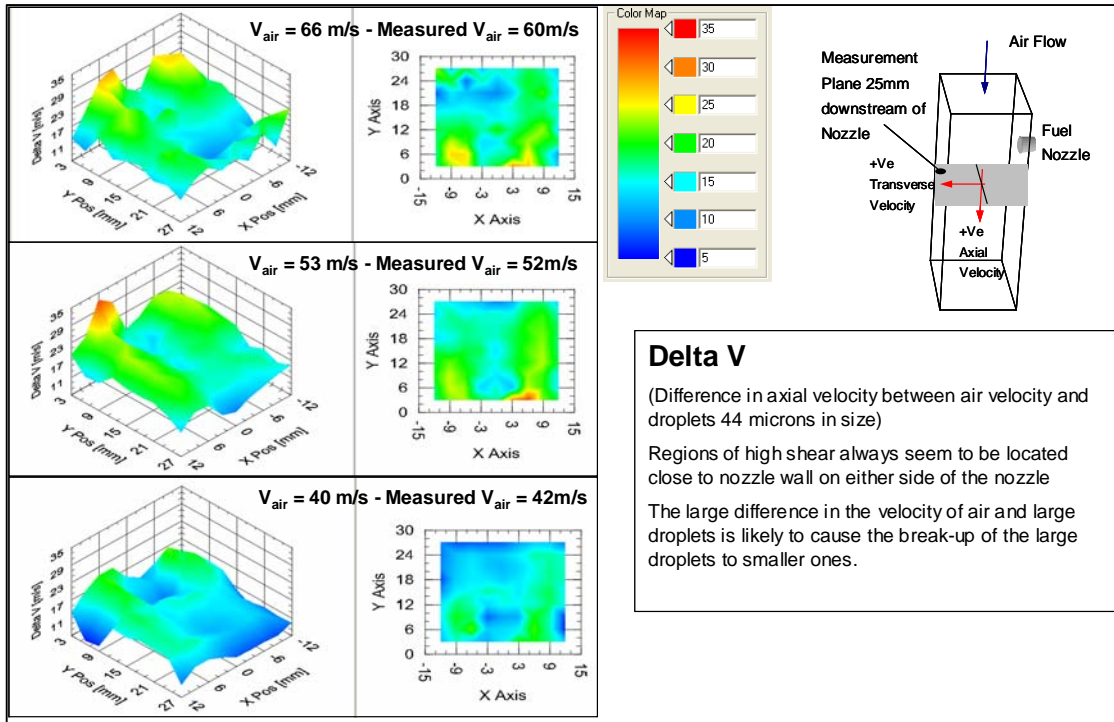


Figure 10. The difference between mean air axial velocity (i.e., the mean axial velocity of droplets < 4 microns compared to the axial velocity of droplets of 44 microns). This gives a qualitative indication of the shear forces experienced by the droplets.

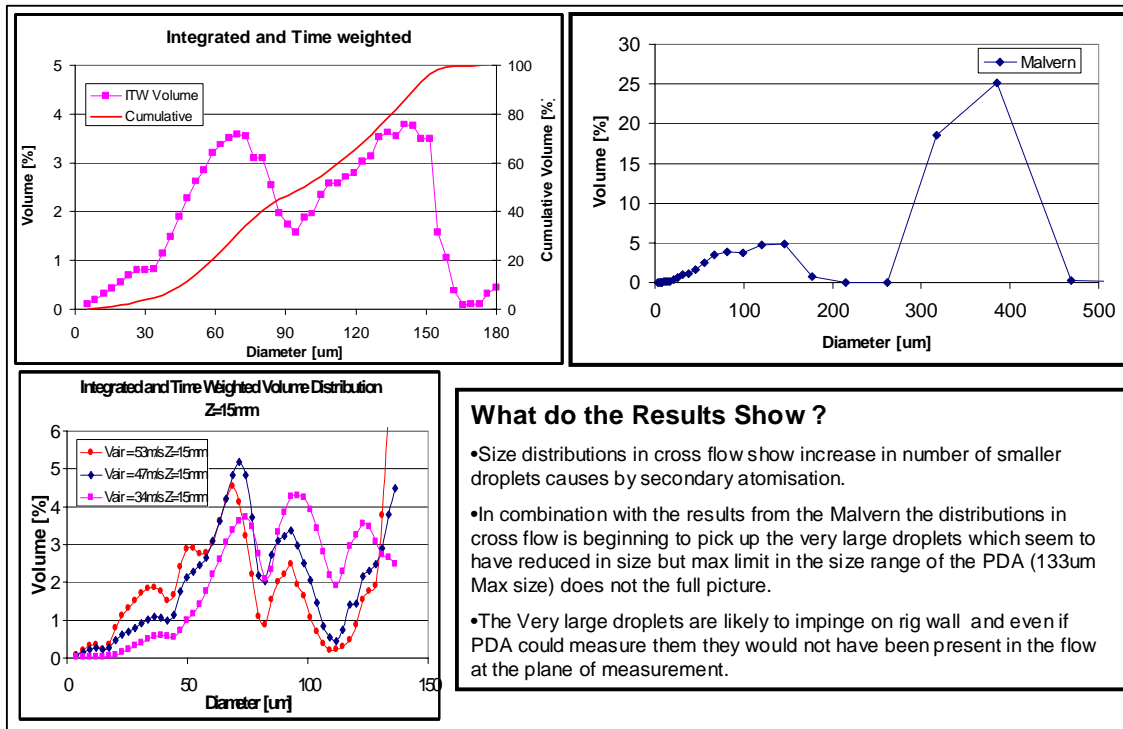


Figure 11. The Malvern Mastersizer X results compared to the integrated and time weighted PDDA results. The larger droplets are not seen by the PDDA instrument but the droplets within the dynamic range of the PDDA agree well with the Malvern results. Further work is being done to verify the Malvern measurements.

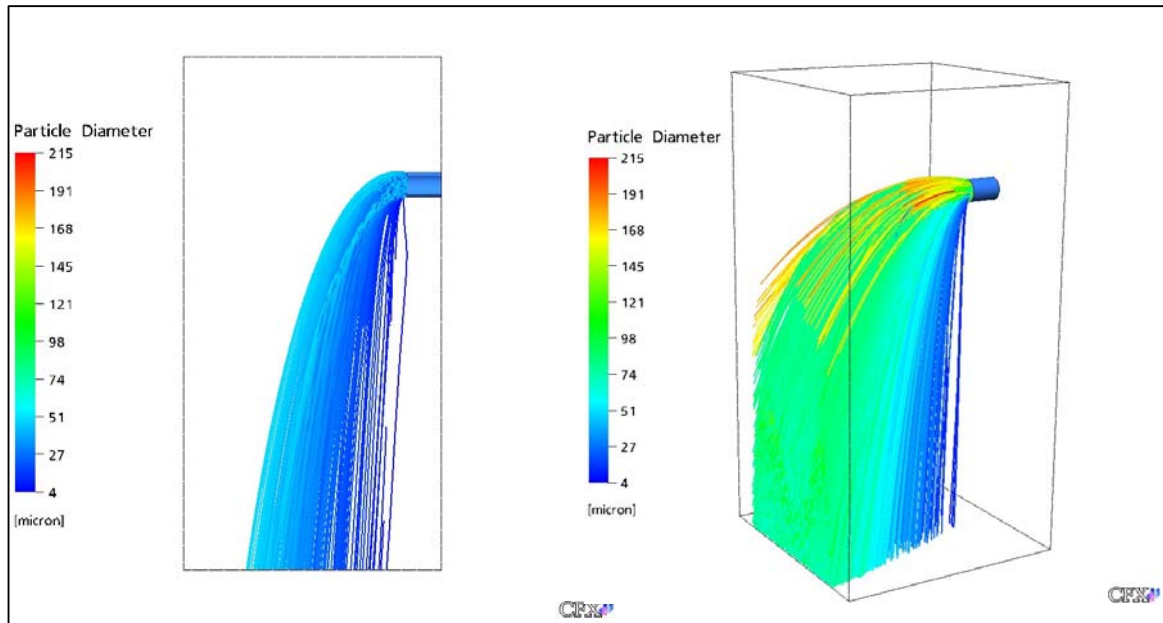


Figure 12. Preliminary CFD results showing the model of the duct. The predicted droplet trajectories for Test Point 1 (mean air flow rate of 66 m/s) are shown.

6.0 REFERENCES

1. Schmehl, R., Maier, G. & Wittig, S., CFD Analysis of Fuel Atomisation, Secondary Droplet Breakup and Spray Dispersion in the Premix Duct of a LPP Combustor, 8th Int. Conf. Liquid Atomisation and Spray System, Pasadena, CA, USA, July 2000
2. CFX 5.7 (April 2004) available from ANSYS Europe Ltd., The Gemini Building, Fermi Avenue, Harwell International Business Centre, Didcot, Oxfordshire, OX11 0QR United Kingdom